



STRUCTURAL
BIOLOGY

Volume 78 (2022)

Supporting information for article:

Native SAD phasing at room temperature

**Jack B. Greisman, Kevin M. Dalton, Candice J. Sheehan, Margaret A. Klureza,
Igor Kurinov and Doeke R. Hekstra**

Table S1. *Peaks in model-phased anomalous difference map of HEWL*

Anomalous Site	Element	Peak height (σ)
Cys6-S $_{\gamma}$	S	16.26
Met12-S $_{\delta}$	S	19.09
Cys30-S $_{\gamma}$	S	22.59
Cys64-S $_{\gamma}$	S	19.29
Cys76-S $_{\gamma}$	S	16.54
Cys80-S $_{\gamma}$	S	20.68
Cys94-S $_{\gamma}$	S	16.46
Met105-S $_{\delta}$	S	21.71
Cys115-S $_{\gamma}$	S	22.15
Cys127-S $_{\gamma}$	S	15.24

Table S2. *Peaks in model-phased anomalous difference map of DHFR*

Anomalous Site	Element	Peak height (σ)
Met42-S $_{\delta}$	S	15.36
Cys85-S $_{\gamma}$	S	12.77
Met92-S $_{\delta}$	S	15.39
NAP202-P2B	P	6.22
NAP202-PA	P	11.91
NAP202-PN	P	11.38
Mn-1	Mn	57.09
Mn-2	Mn	4.24
Mn-3	Mn	22.08
Mn-4	Mn	10.39
Mn-5	Mn	10.22

Table S3. *Peaks in model-phased anomalous difference map of apo PTP1B*

Anomalous Site	Element	Peak height (σ)
Met74-S $_{\delta}$	S	12.03
Met98-S $_{\delta}$	S	20.48
Met109-S $_{\delta}$	S	22.78
Met114-S $_{\delta}$	S	11.60
Cys121-S $_{\gamma}$	S	14.39
Met133-S $_{\delta}$	S	13.73
Cys215-S $_{\gamma}$	S	24.45
Cys226-S $_{\gamma}$	S	15.46
Cys231-S $_{\gamma}$	S	19.05
Met235-S $_{\delta}$	S	8.43
Met253-S $_{\delta}$	S	14.04
Met258-S $_{\delta}$	S	16.54
Met282-S $_{\delta}$	S	6.28

Table S4. *Peaks in model-phased anomalous difference map of PTP1B:TCS401 complex*

Anomalous Site	Element	Peak height (σ)
Met3-S δ	S	6.84
Met74-S δ	S	11.35
Met98-S δ	S	19.39
Met109-S δ	S	21.44
Met114-S δ	S	11.65
Cys121-S γ	S	21.87
Met133-S δ	S	13.26
Cys215-S γ	S	20.72
Cys226-S γ	S	14.72
Cys231-S γ	S	18.33
Met235-S δ	S	8.68
Met253-S δ	S	13.75
Met258-S δ	S	15.40
Met282-S δ	S	11.30
OTA301-S13	S	21.84

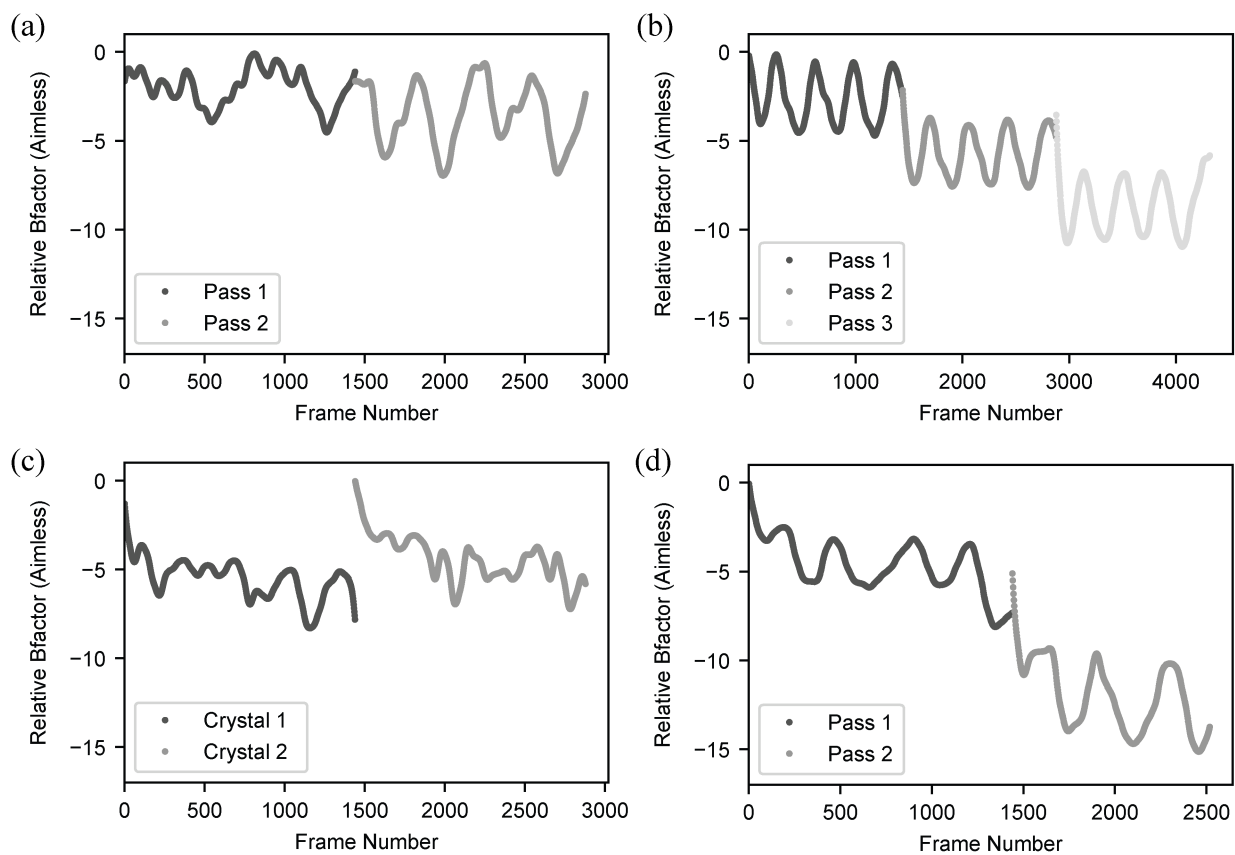


Fig. S1. **Relative image B-factors emphasize limited radiation damage.**

Image B-factors fit during scaling in *AIMLESS* are an indicator of radiation damage. Values significantly below -10 are often considered a sign of damage (Evans & Murshudov, 2013). The image B-factors are presented for the datasets collected on each crystal for (a) HEWL, (b) DHFR, (c) apo PTP1B, and (d) PTP1B:TCS401 complex. Although the image B-factors for the final passes on DHFR and PTP1B:TCS401 reach values lower than -10, excluding such frames from the analysis was not found to improve the SAD phasing results (not shown).

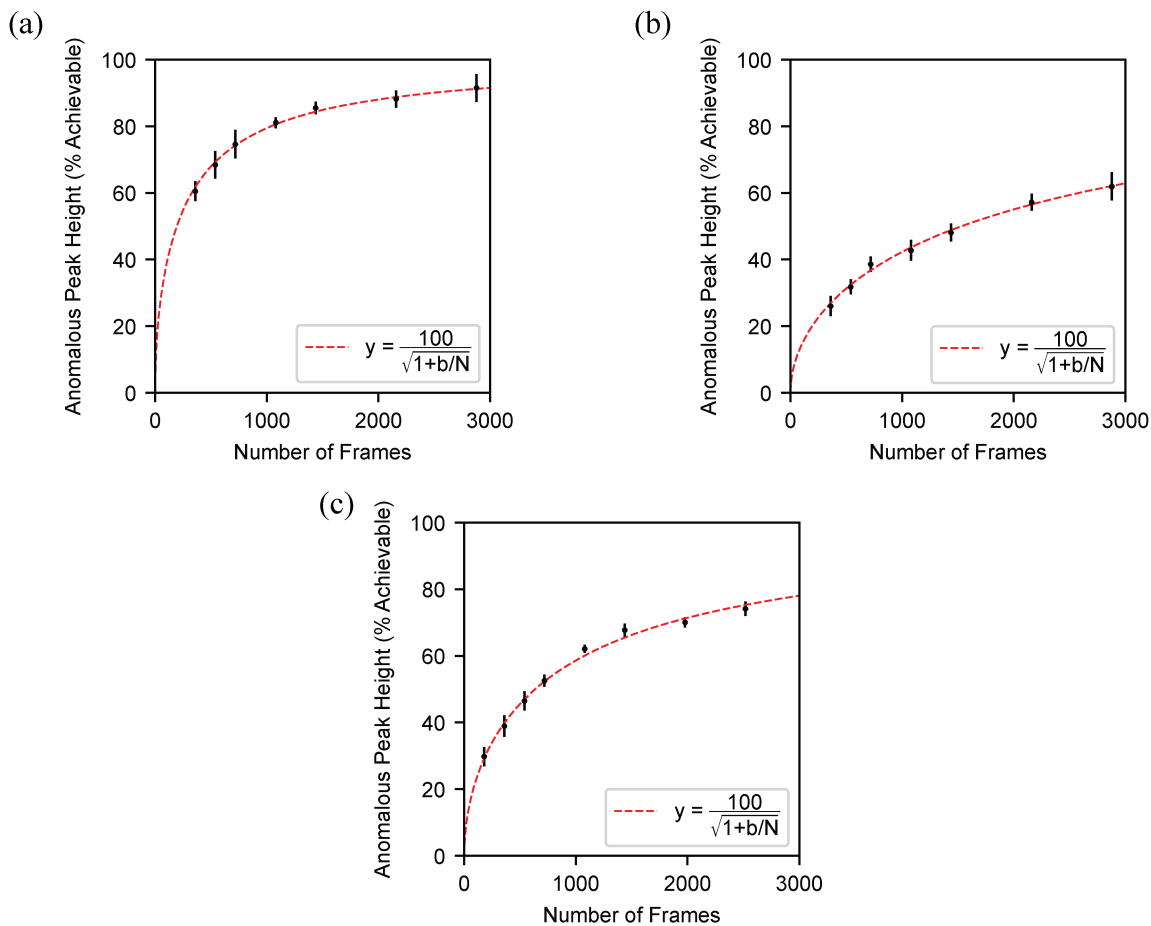


Fig. S2. **Redundancy improves anomalous signal for native SAD datasets.**

Anomalous peak heights corresponding to the anomalous sites in the asymmetric unit cell after refinement using merged intensities for datasets with different numbers of frames are shown for (a) DHFR, (b) apo PTP1B, and (c) PTP1B:TCS401 complex (black data points; mean \pm standard deviation). The peak heights are on an absolute scale relative to the maximal value that can be achieved. A non-linear least-squares fit to the data is shown for $y = 100/\sqrt{1+b/N}$ (red dashed line). This analysis only includes the anomalous sites that could be identified in all anomalous difference maps for the subsets of the data. The values fit for b are (a) 583 ± 48 , (b) 4620 ± 1140 , and (c) 1900 ± 250 (95% confidence interval).

Table S5. *Figure of Merit from Native SAD Phasing of HEWL*

Number of Frames	Figure of Merit
180	0.23
360	0.24
720	0.40
1439	0.44
2159	0.46
2878	0.47